Functionalized planar aromatic rings as precursors to energetic N,N'-(4,6-dinitro-1,3-phenylene)dinitramide and its salts

Journal:	*Materials Chemistry Frontiers*
Manuscript ID	QM-RES-02-2022-000092.R1
Article Type:	Research Article
Date Submitted by the Author:	14-Feb-2022
Complete List of Authors:	Shreeve, Jean'ne; University of Idaho, Chemistry Singh, Jatinder; University of Idaho, Chemistry; Indian Institute of Technology Delhi, Lal, Sohan; University of Idaho, Chemistry Staples, Richard; Michigan State University, Chemistry

ARTICLE

Functionalized planar aromatic rings as precursors to energetic N,N'-(4,6-dinitro-1,3-phenylene)dinitramide and its salts

Jatinder Singh,[a] Sohan Lal,[a] Richard J. Staples,[b] Jean'ne M. Shreeve[a]*

Received 00th January 20xx,
Accepted 00th January 20xx

DOI: 10.1039/x0xx00000x

Functionalization of planar aromatic rings is very straightforward, up scalable, and economical in comparison with many azole, caged, linear or cyclic structures. In our present work, a facile synthesis of N,N'-(4,6-dinitro-1,3-phenylene)dinitramide (**3**) is obtained by a single-step nitration of 4,6-dinitrobenzene-1,3-diamine (**2**). Compound **3** exhibits a surprisingly high density of 1.90 g cm^{-3} at 100 K (1.87 g cm^{-3} at 298 K). Its reactions with bases result in the formation of a series of energetic salts (**4**-**7**) which exhibit relatively high densities (1.74 to 1.83 g cm^{-3}), and acceptable thermal sensitivities (177 to 253 °C). Energetic salt formation increases intermolecular hydrogen bonding while the planarity of the aromatic ring maximizes weak non-covalent interactions (π-stacking, cation/π, anion-π, X-H/π, etc.,). The synergetic effect of these stabilizing interactions play a crucial role in increasing thermal stability and decreasing sensitivity toward the external stimuli. Overall, these easily accessible new energetic compounds exhibit high densities and good denotation properties with potential applications as new high-energy materials.

Traditional energetics based on planar aromatic rings have been used widely in military, industrial, and mining applications.[1] Among them, TATB (1,3,5-triamino-2,4,6-trinitrobenzene) is an energetic material which has been authorized by the U.S. Department of Energy due to its low sensitivity to impact, friction and spark, and good decomposition power.[2] TNT (2,4,6- trinitrotoluene) is another commonly used energetic material based on its melt-castable properties for safe transportation and storage.[3] However, the minimal detonation properties of TATB and TNT make them less desirable in comparison to the nitroamine-based energetic materials such as RDX (1,3,5-trinitro-1,3,5-triazinane), HMX (1,3,5,7-tetranitro-1,3,5,7-tetrazocane), and CL-20 (2,4,6,8,10,12-hexanitro-2,4,6,8,10,12-hexaazaisowurtzita--itane).[4] The presence of nitrogen-oxygen-rich nitroamine (>NNO_2) groups enhances density.[5] For instance, HMX has an additional $CH_2N(CH_2)NO_2$ unit relative to RDX, which results in an increase in density from 1.80 g cm^{-3} to 1.90 g cm^{-3}, and concomitantly in detonation velocity from 8795 m s^{-1} to 9144 m s^{-1}).[6] However, the synthesis of energetic materials containing nitro ($-NO_2$), nitroamino ($-NHNO_2$), and azido ($-N_3$), present a formidable challenge due to a trade-off between high density and molecular stability.[7]

In recent years, the application of high energy density materials (HEDMs) has been one of the hot spots in the field of energy materials.[8] These HEDMs utilize nitrogen-rich heterocycles in combination with energetic explosophores to achieve superior properties.[9] However, the high cost of large-scale syntheses and overall poor yields very often limit their practical applicability.[10] To this end, the search for easily accessible materials with high densities, in combination with acceptable thermal stabilities, is necessary in order to realize the acquisition of new energetic materials. By examining the molecular structure of energetic materials based on azole, caged, linear or cyclic structures, we note that functionalization of the planar aromatic rings is very straightforward, up scalable, and economical.[11 a]

The introduction of $-NHNO_2$ groups onto a planar aromatic ring enhances the density and energetic properties.[12] In addition, the planarity of this ring maximizes weak non-covalent interactions (π-stacking, cation/π, anion-π, X-H/π, etc.,), which play vital roles in increasing thermal stability and decreasing the sensitivity toward the external stimuli. The synergetic effect of multiple weak non-covalent interactions is important in constructing a molecule with high stability and is a markedly attractive concept in the synthesis of high energy materials. Therefore, the thermally stable 4,6-dinitrobenzene-1,3-diamine, which is obtained in a few steps in excellent yield from easily available starting materials was selected for study.[13] In a continuation of our ongoing interest in the development of new energetic materials, we have synthesized by the N-nitration of 4,6-dinitrobenzene-1,3-diamine and characterized N,N'-(4,6-

---

[a] *Department of Chemistry, University of Idaho, Moscow, Idaho, 83844-2343, United States.*
[b] *Department of Chemistry, Michigan State University, East Lansing, Michigan 48824, United States.*

Electronic Supplementary Information (ESI) available: For ESI and crystallographic data in CIF or other electronic format see DOI: 10.1039/x0xx00000x dinitro-1,3-phenylene)dinitramide, **3**, and its salts. The reaction of hydrazine hydrate with 1,5-dichloro-2,4-dinitrobenzene, **1**, resulted in the formation of (4,6-dinitro-1,3-phenylene)bis(hydrazine), **8**, in excellent yield. These materials exhibit relatively high densities, high heats of formation, and acceptable thermal sensitivities.

Results and Discussion

Synthesis

Compounds **1** and **2** were synthesized based on the literature.[13] The reaction of 4,6-dinitrobenzene-1,3-diamine, **2**, with red fuming nitric acid results in the formation of N,N'-(4,6-dinitro--1,3-phenylene)dinitramide, **3**, as a brown solid in 85% yield (Scheme 1). Since energetic salt formation decreases sensitivity and enhances thermal stability, compound **3** was reacted with various nitrogen-rich bases in acetonitrile to give 1:2 salts. In addition, the reaction of hydrazine hydrate with 1,5-dichloro-2,4-dinitrobenzene, **1**, resulted in the formation of (4,6-dinitro-1,3-phenylene)bis(hydrazine), **8**, in excellent yield (Scheme 1).

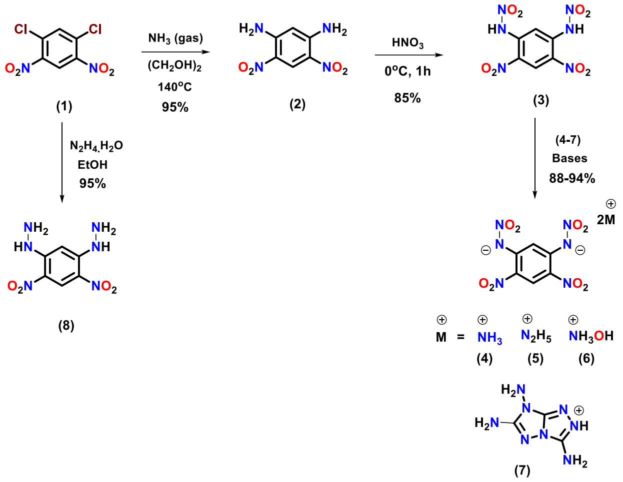

Scheme 1: Synthesis of N,N'-(4,6-dinitro-1,3-phenylene)dinitramide (**3**) and its energetic salts (**4-7**).

Spectral studies of compounds

All compounds have been fully characterized by NMR [^{1}H, ^{13}C{^{1}H}, and ^{15}N{^{1}H}] and IR spectra as well as elemental analysis. In the ^{1}H NMR of compounds **3**-**7**, a phenyl proton neighboring the nitroamine groups shows a downfield shift, while a phenyl proton neighboring the nitro groups has an upfield shift in comparison to the corresponding 4,6-dinitrobenzene-1,3-diamine (**2**).

In the ^{13}C{^{1}H} NMR spectra, signals corresponding to the ring carbon atoms attached to nitroamine groups in compounds **3–7** were observed in the range of 139.4 to 146.8 ppm and the carbon atoms attached to nitro groups were observed over the range of 134.7 to 135.9 ppm. The ^{15}N NMR spectra of **5** and **7** are given in Figure 1. In the spectrum of **5,** three signals are seen for the nitrogen atoms of the dianion at δ = -126.5 (N1), -7.7 (N2), -15.7 (N3) ppm, while nitrogen atoms corresponding to compound **7** are seen at δ = -139.3 (N1), -8.9 (N2), -17.9 (N3) ppm.

Crystal structure

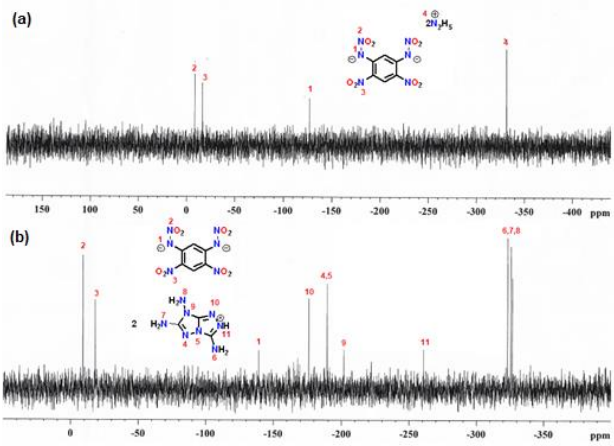

Figure 1: ^{15}N NMR spectra of (a) **5,** (b) **7**.

Suitable crystals were obtained for **3**, **5** and **7** by slow evaporation of their saturated solutions in methanol/acetonitrile or methanol/water mixtures, and their crystal structures are given in Figures 2-4. Crystallographic data and data collection parameters, bond lengths, and bond angles are given in the ESI.† Compound **3** crystallizes in the orthorhombic space group $Pca2_1$ with a calculated density of 1.907 g cm^{-3} at 100K. As shown in Figure 2c, the crystal framework of **3** shows a herringbone packing of planar rings. The nitroamine and nitro groups of **3** are involved in inter- and intra-hydrogen bonding interactions, which make a positive contribution to the density. The C-N bond lengths in C-NHNO$_2$

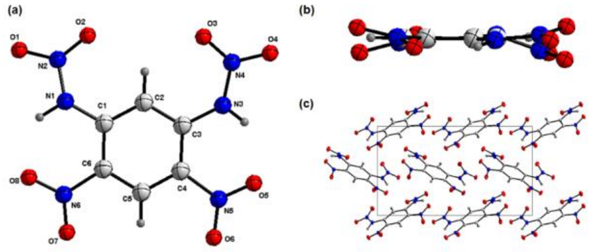

Figure 2: (a) and (b) Thermal ellipsoid plot (50%) and labeling scheme for **3**. (c) Ball-and-stick packing diagram of **3**.

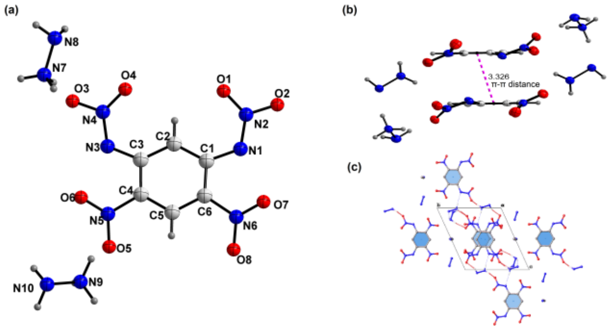

Figure 3: (a) and (b) Thermal ellipsoid plot (50%) and labeling scheme for **5**. (c) Ball-and-stick packing diagram of **5**. Solvent molecule has been removed from Fig. 3a and Fig. 3b for clarity.

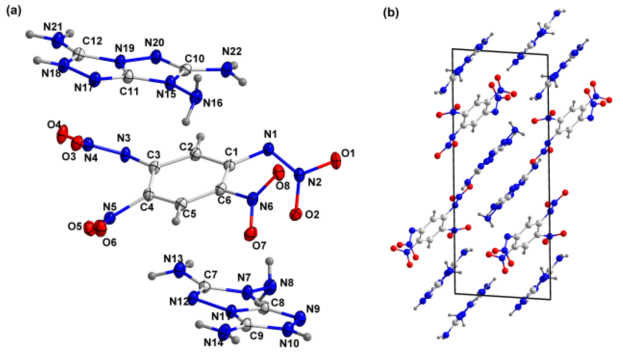

Figure 4: (a) Thermal ellipsoid plot (50%) and labeling scheme for **7**. (b) Ball-and-stick packing diagram of **7**.

groups [C1-N1, 1.392(3) Å and C3-N3, 1.394(3) Å] are shorter than those of C-NO_2 groups [C4-N5, 1.460(3) Å and C6-N6, 1.462(3) Å].

Compound **5**·0.5CH_3CN belongs to the triclinic space group *P-1*, with a calculated density of 1.736 g cm^{-3} at 100K. The compound crystallizes with acetonitrile molecules in the lattice, which results in deceased crystal density. As shown in Figure 3b, the crystal framework of **5**·0.5CH_3CN shows a face-to-face packing of planar rings, which give rise to π-π interactions (3.326 Å). The nitroamine and nitro groups of **5**·0.5CH_3CN form intermolecular hydrogen bonding interactions with hydrazinium ions, which is helpful in improving the stability of the molecule. The crystal packing of compound **5**·0.5CH_3CN can be viewed as a face-to-face arrangement of planar rings (Figure 3c). The C-N bond lengths in C-$NHNO_2$ groups [C1-N1, 1.404(3) Å and C3-N3, 1.404(3) Å] are shorter than that of C-NO_2 groups [C4- N5, 1.463(3) Å and C6-N6, 1.460(3) Å].

Compound **7** belongs to the triclinic space group *P-1*, with a calculated density of 1.800 g cm^{-3} at 100K. The dianion is sandwiched between two cations forming a triple decker structure (Figure 4). As shown in Figure 4b, the crystal framework of **7** shows a face-to-face packing of three rings, which give rise to π-π interactions (3.289-3.394 Å). The stabilizing interactions such as O···H, N···H and H···H are observed in the crystal packing of **7**, which are helpful in improving the overall stability of the molecule.

Hirshfeld surface and non-covalent interactions

Since crystal packing strongly influences physical properties of energetic compounds, two-dimensional (2D) fingerprints and the associated Hirshfeld surfaces[14,15] were employed by using Crystalexplorer17.5 to understand structure-properties and intermolecular interactions in **3**, **5**·0.5CH_3CN and **7** (Figure 5). Red and blue dots on the Hirshfeld surface analysis represent high and low close contacts. In Figure 5a-5c, strong intermolecular (O···O) interactions arising from oxygen atoms in nitroamine, and nitro groups are shown in **3**, leading to high density and higher sensitivity to external stimuli. The calculated results show the O···O contact interactions of **3** accounts for 30.7%, which is much higher than the stabilizing interactions such as O···H (23.6%) and N···H (0.1%) known to decrease the mechanical sensitivity. In contrast to **3**, the O···O contact interactions of **5**·0.5CH_3CN and **7** accounts are only 6.5% and 2.2 %, respectively, which are much smaller in comparison to the other stabilizing interactions. The stabilizing O···H and N···H interactions are seen in **5**·0.5CH_3CN, which contribute to the total weak interactions of 56.8%. In contrast, compound **7** exhibits a surprisingly high percentage (69.9%) of O···H and N···H interactions. As shown in Figure 5f and 5i, high percentages of N···N, and N···C interactions were observed which denote π–π stacking for **5**·0.5CH_3CN and **7**. This is also supported by noncovalent interaction (NCI) plots of gradient isosurfaces for **5**·0.5CH_3CN and **7** (Figure 6). The green surface can be clearly seen from the Figure 6a and 6b due to the presence of π-π interactions.[16] The combination of N···H, O···H and π-π interactions leads to the insensitivity and high molecular stability of compounds **5**·0.5CH_3CN, and **7** (Figure 6). The calculated results are in excellent agreement with the sensitivity data from experiment, which show impact sensitivities of **5**·0.5CH_3CN, and **7** are 22 J and 25 J, respectively.

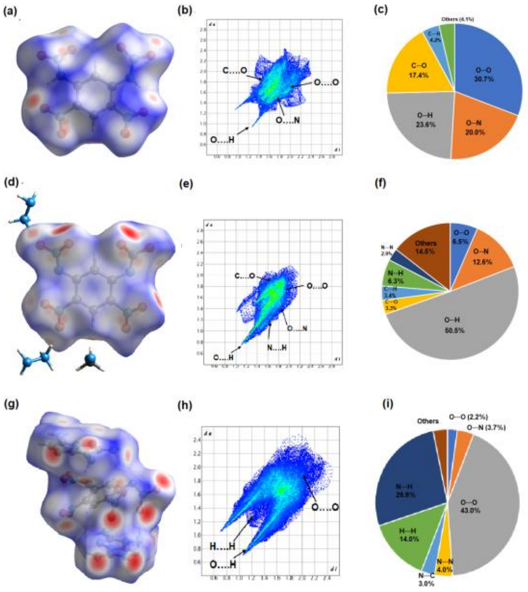

Figure 5: Hirshfeld surface graphs and 2D fingerprint plots of compounds **3** (a,b,c), **5**·0.5CH_3CN (d,e,f), and **7** (g,h,i).

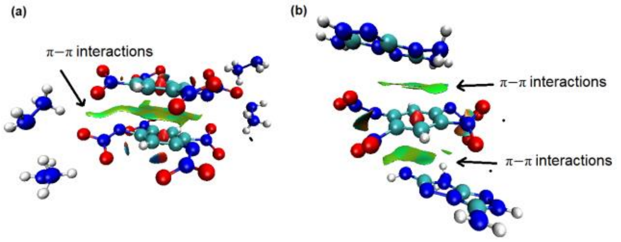

Figure 6: Non-covalent interaction plots of gradient isosurfaces for (a) **5**·0.5CH_3CN, and (b) **7**.

Physicochemical and energetic properties

Table 1: Energetic properties of compounds 3-8.

	ρ^a g cm^{-3}	$\Delta H_f{}^b$ kJmol^{-1}/kJg^{-1}	$\Delta H_f{}^c$ kJmol^{-1}/kJg^{-1}	$D_v{}^d$ m s^{-1}	P^e GPa	$T_d{}^f$ °C	IS^g J	FS^h N	OB^i %
3	1.87	112.5/0.49	149.4/0.52	8644/8682	33.7/34.0	125	7	120	-33.3
4	1.74	80.6/0.25	286.7/0.88	8409/8575	29.5/31.3	195	25	160	-140.1
5	1.77	362.2/1.02	578.3/1.64	8834/8992	32.6/34.3	177	22	160	-45.4
6	1.83	231.9/0.65	365.5/1.03	8890/8980	36.7/37.7	176	25	160	-140.1
7	1.76	1277.9/2.14	1277.3/2.14	8525/8525	28.3/28.3	253	25	240	-64.4
8	1.72	163.93/0.72	239.7/1.05	8016/8121	24.1/24.9	258	35	>240	-84.1
TATB[j]	1.94	-154.2/0.59	-	8201	28.0	360	50	>360	-55.8
HMX[k]	1.91	105.0/0.35	-	9144	39.2	280	7	120	-21.6
RDX[k]	1.80	92.6/0.42	-	8795	34.9	204	7.5	120	-21.6

[a] Density – gas pycnometer at 25 °C. [b] Calculated molar enthalpy of formation (Isodesmic method). [c] Calculated molar enthalpy of formation (Atomization method). [d] Calculated detonation velocity (isodecmic/atomization). [e] Calculated detonation pressure (isodecmic/atomization). [f] Temperature of decomposition (onset). [g] Impact sensitivity. [h] Friction sensitivity. [i] Oxygen balance based on CO_2. For a compound with the molecular formula of $C_aH_bN_cO_d$, Ω_{CO2} (%) = $1600[(d - 2a - b/2)/MW]$, where MW is the molecular weight. [j] Ref. 17. [k] Ref. 18. All compounds were obtained as anhydrous powders (confirmed by elemental analysis) to determine the properties in Table 1.

The thermal stabilities of new energetic materials **3**–**8**, were determined using differential scanning calorimetry (DSC) at a heating rate of 5 °C min^{-1} (Table 1). The decomposition temperatures for all compounds occur between 176 (**6**) and 258 (**8**) °C, except for compound **3** which decomposes at 125 °C. The densities were measured using a gas pycnometer at 25 °C and the values range between 1.72 (**8**) to 1.87 (**3**) g cm^{-3}. The heats of formation of compounds **3–8** were calculated based on isodesmic reactions and as well as the atomization method using the Gaussian 03 (revision D.01) suite of programs (SI).[19] All the compounds have relatively high positive heats of formation (ΔH_f), and are significantly higher than both RDX (92.6 kJ mol^{-1}) and HMX (105.0 kJ mol^{-1}). Based on the values of calculated heats of formation and experimental densities, detonation properties of compounds **3–8** were determined using EXPLO5 (version 6.01). Compounds **5** and **6** have better detonation properties than RDX (Table 1). Impact and friction sensitivity values were obtained by using a BAM drop hammer apparatus and BAM friction tester, respectively. Except for compound **3**, all the compounds were found to have good sensitivities (IS > 20 J, FS > 120 N) to both impact and friction.

Conclusions

New energetic compounds **3**-**8** have been designed and synthesized from readily accessible starting materials, 1,5-dichloro-2,4-dinitrobenzene and 4,6-dinitrobenzene-1,3-diamine, in a minimum number of steps in good yields. All new compounds were characterized by advanced spectroscopic techniques. Single-crystal X-ray diffraction analysis was used to confirm the structures of **3**, **5**·$0.5CH_3CN$, and **7**. In addition to their efficient syntheses, all compounds exhibit high densities (1.72 to 1.87 g cm^{-3} at 298K), good thermal stabilities (125-258 ºC), acceptable sensitivities, and good detonation properties. The synergetic effect of multiple weak non-covalent interactions is found to be effective in increasing the molecular stability of these compounds. These easily accessible energetic materials with high detonation properties may provide good alternatives to RDX.

Experimental section

Caution! Although no explosions or hazards were observed during the preparation and handling of these compounds, all the compounds investigated are energetic materials. Mechanical actions involving scratching or scraping must be avoided. In addition, all the compounds must be synthesized on a small scale. All manipulations should be carried out in a hood behind a safety shield. Eye protection and leather gloves must be worn at all times.

General methods

All reagents were purchased from VWR or AK Scientific in analytical grade and were used as supplied, if not stated otherwise. ^1H and ^{13}C NMR spectra were recorded using a 300 MHz (Bruker AVANCE 300) NMR spectrometer operating at 300.13 and 75.48 MHz, respectively. A 500 MHz (Bruker AVANCE 500) NMR spectrometer operating at 50.69 MHz was used to obtain ^{15}N NMR spectra. Chemical shifts in the ^1H and ^{13}C NMR spectra are reported relative to Me_4Si and ^{15}N NMR spectra to $MeNO_2$. The melting and decomposition (onset) points were obtained on a differential scanning calorimeter (TA Instruments Company, Model: Q2000) at a scan rate of 5 °C min^{-1}. IR spectra were recorded on a FT-IR spectrometer (Thermo Nicolet AVATAR 370) as thin films using KBr plates. Density was measured at room temperature by employing a Micromeritics AccuPyc II 1340 gas pycnometer. The impact (IS) and friction sensitivities (FS) were measured with a standard BAM drop hammer and BAM friction tester. Elemental analyses (C, H, N) were determined using a Vario Micro cube Elementar Analyser.

Orange block crystals of **3** with dimensions 0.11 × 0.09 × 0.06 mm^3, yellow block crystals of **5**·$0.5CH_3CN$ with dimensions 0.07 × 0.05 × 0.02 mm^3 and yellow needle crystals of **7** with dimensions 0.20 × 0.04 × 0.03 mm^3 were selected and mounted on a nylon loop with Paratone oil on a XtaLAB Synergy, Dualflex, HyPix diffractometer. The crystals were kept at a steady T = 100.00(10) K during data collection. The structures were solved with the ShelXT[20] solution program using dual methods and by using Olex2.[21] The model was refined with ShelXL[22] using full matrix least squares minimization on F^2.

Theoretical study

The heats of formation for compounds **3**-**8** were obtained by using isodesmic reactions and atomization method (ESI†). The geometric optimization and frequency analyses of the structures are based on available single crystal structures and using the B3LYP functional with the 6-31+G** basis set. Single-point energies were calculated at the MP2/6-311++G** level.[23] Atomization energies for cations were obtained by employing the G^2*ab initio* method.[24] All of the optimized structures were characterized to be true local energy minima on the potential energy surface without imaginary frequencies. For energetic salts, the solid-phase heats of formation were calculated based on the Born–Haber energy cycle.[25] All calculated gas-phase enthalpies for covalent materials are converted to solid phase values by subtracting the empirical heat of sublimation obtained based on Trouton's rule.[26]

Synthesis of N,N'-(4,6-dinitro-1,3-phenylene)dinitramide (3)

To red fuming acid (1 mL), stirred at 0 °C, was added 4,6-dinitrobenzene-1,3-diamine[13] (0.20 g, 1.01 mmol) in small portions. Stirring was continued at the same temperature for 1h and the mixture was poured into ice (20 g). The resulting brown precipitate was filtered and washed with water (3 x 20 mL). Yield: 85%; T_m (onset) = 125 °C; ^{1}H NMR (300 MHz, d_6-DMSO, ppm): 8.66 (s, 1H), 7.69 (s, 1H), 4.92 (bs, N*H*); ^{13}C NMR (75 MHz, d_6-DMSO, ppm): 139.4, 134.7, 123.5, 122.8; IR (*v*, cm^{-1}): 3261, 3081, 1577, 1534, 1395, 1286, 1078, 997, 910, 835, 738, 590. Elemental analysis: Calcd (%) for $C_6H_4N_6O_8$ (288.13): C, 25.01; H, 1.40; N, 29.17; Found: C 25.51, H 1.64, N 27.20.

General procedure for the synthesis of energetic salts (**4-7**)

Aqueous ammonia, hydrazine hydrate, hydroxylamine or 3,6,7-triamino-7*H*-[1,2,4]triazolo[4,3-*b*][1,2,4]triazol-2-ium) (2.0 mmol) was added to a suspension of **3** (1.0 mmol) in CH_3CN (10 mL). The precipitate was collected by filtration to give the product, which was purified further by washing with CH_3CN (3 x 10 mL).

Diammonium (4,6-dinitro-1,3-phenylene)bis(nitroamide) (4): Yield: 92%; T_d (onset) = 195 °C; ^{1}H NMR (300 MHz, d_6-DMSO, ppm): 8.18 (s, 1H), 7.17 (s, 8H), 7.02 (s, 1H); ^{13}C NMR (75 MHz, d_6-DMSO, ppm): 146.7, 135.6, 121.3, 119.0; IR (*v*, cm^{-1}): 3035, 1548, 1444, 1337, 1223, 980, 897, 827, 755, 554; Elemental analysis: Calcd (%) for $C_6H_{10}N_8O_8$ (322.19): C, 22.37; H, 3.13; N, 34.78; Found: C 22.44, H 3.36, N 32.93.

Dihydrazinium (4,6-dinitro-1,3-phenylene)bis(nitroamide) (5): Yield: 90%; T_d (onset) = 184 °C; ^{1}H NMR (300 MHz, d_6-DMSO, ppm): 8.17 (s, 1H), 7.02 (s, 1H), 6.85 (s, 10H); ^{13}C NMR (75 MHz, d_6-DMSO, ppm): 146.8, 135.7, 121.3, 119.1; IR (*v*, cm^{-1}): 3092, 1592, 1503, 1291, 1098, 1017, 975, 902, 832, 759; Elemental analysis: Calcd (%) for $C_6H_{12}N_{10}O_8$ (352.22): C, 20.46; H, 3.43; N, 39.77; Found: C 20.24, H 3.87, N 39.06.

Dihydroxylammonium(4,6-dinitro-1,3-phenylene)bis(nitro-amide) (6): Yield: 94%; T_d (onset) = 176 °C; ^{1}H NMR (300 MHz, d_6-DMSO, ppm): 8.20 (s, 1H), 8.13 (s, 6H), 7.04 (s, 1H); ^{13}C NMR (75 MHz, d_6-DMSO, ppm): 146.6, 135.8, 121.4, 119.2; IR (*v*, cm^{-1}): 3040, 1607, 1530, 1329, 986, 908, 831, 761, 723, 588; Elemental analysis: Calcd (%) for $C_6H_{10}N_8O_{10}$ (354.19): C, 20.35; H, 2.85; N, 31.64; Found: C 20.93, H 3.52, N 31.34.

Di(3,6,7-triamino-7*H*-[1,2,4]triazolo[4,3-*b*][1,2,4]triazol-2-ium)(4,6-dinitro-1,3-phenylene)bis(nitroamide) (7): Yield: 88%; T_d (onset) = 195 °C; ^{1}H NMR (300 MHz, d_6-DMSO, ppm): 8.75 (s, 2H), 8.44 (s, 1H), 8.25 (s, 4H), 7.60 (s, 1H), 6.22 (bs, 8H); ^{13}C NMR (75 MHz, d_6-DMSO, ppm): 152.2, 147.8, 142.3, 140.8, 136.3, 122.0, 120.2; IR (*v*, cm^{-1}): 3565, 3137, 1690, 1607, 1527, 1339, 1279, 1084, 1023, 913, 837, 757, 708, 593; Elemental analysis: Calcd (%) for $C_{12}H_{16}N_{22}O_8$ (596.40): C, 24.17; H, 2.70; N, 51.67; Found: C, 23.76; H, 2.61; N, 48.02.

(4,6-Dinitro-1,3-phenylene)bis(hydrazine) (8)

To a mixture of 1,5-dichloro-2,4-dinitrobenzene (1.00 g, 4.21 mmol) in ethanol (30 mL) was added hydrazine hydrate (10 mmol) dropwise. The reaction mixture was heated at 80 ºC for 3 h. The orange precipitate was filtered and washed with ethanol (3 x 20 mL) and water (3 x 20 mL). Yield: 95%; T_d (onset) = 258 °C; ^{1}H NMR (300 MHz, d_6-DMSO, ppm): 9.29 (s, 2H), 8.88 (s, 1H), 7.19 (s, 1H), 4.74 (s, 4H); ^{13}C NMR (75 MHz, d_6-DMSO, ppm): 149.6, 128.5, 122.6, 91.0; IR (*v*, cm^{-1}): 3353, 3223, 3080, 1644, 1587, 1528, 1479, 1398, 1288, 1239, 1201, 1042, 989, 840, 743, 700; Elemental analysis: Calcd (%) for $C_6H_8N_6O_4$ (228.17): C, 31.58; H, 3.53; N, 36.83; Found: C 31.66, H 3.75, N 36.07.

Acknowledgements

The Rigaku Synergy S Diffractometer was purchased with support from the MRI program of the National Science Foundation (Grant no. 1919565).

References

1 (a) D. Kumar and A. J. Elias, The Explosive Chemistry of Nitrogen, *Resonance*, 2019, **24**, 1253–1271; (b) W.-L. Yuan, G.-H. Tao, L. Zhang, Z. Zhang, Y. Xue, L. He, J. Huang and W. Yu, Super Impact Stable TATB Explosives Recrystallized by Bicarbonate Ionic Liquids with a Record Solubility, *Sci. Rep*., 2020, **10**, 4477.

2 H. Ritter and H. H. Licht, Synthesis and Characterization of Methylnitramino-Substituted Pyridines and Triazines, *Propellants, Explos. Pyrotech*., 1993, **18**, 81–88.

3 K. G. Balachandar and A. Thangamani, Design of New Energetic Materials Based on Derivatives of 1,3,5-Trinitrobenzenes: A Theoretical and Computational Prediction of Detonation Properties, Blast Impulse and Combustion Parameters, *Heliyon*, 2020, **6**, e03163.

4 (a) V. A. Strunin and L. I. Nikolaeva, Combustion Mechanism of RDX and HMX and Possibilities of Controlling the Combustion Characteristics of Systems Based on Them, Combust. *Explos. Shock Waves*, 2013, **49**, 53–63; (b) A. E. D. M. van der Heijden and R. H. B. Bouma, Crystallization and Characterization of RDX, HMX, and CL-20, *Cryst. Growth Des*., 2004, **4**, 999–1007; (d) O. Bolton, L. R. Simke, P. F. Pagoria and A. J. Matzger, High Power Explosive with Good Sensitivity: A 2:1 Cocrystal of CL-20:HMX, *Cryst. Growth Des*., 2012, **12**, 4311–4314; (c) D. Chakraborty, R. P. Muller, S. Dasgupta and W. A. Goddard, The Mechanism for Unimolecular Decomposition of RDX (1,3,5-Trinitro-1,3,5-Triazine), an Ab Initio Study, *J. Phys. Chem. A*, 2000, **104**, 2261–2272; (d) J. Yang, G. Wang, X. Gong, J. Zhang and Y. A. Wang, High-Energy Nitramine Explosives: A Design Strategy from Linear to Cyclic to Caged Molecules, *ACS Omega*, 2018, **3**, 9739–9745.

5 M. Reichel, D. Dosch, T. Klapötke and K. Karaghiosoff, Correlation between Structure and Energetic Properties of Three Nitroaromatic Compounds: Bis(2,4-Dinitrophenyl) Ether, Bis(2,4,6-Trinitrophenyl) Ether, and Bis(2,4,6-Trinitrophenyl) Thioether, *J. Am. Chem. Soc*., 2019, **141**, 19911–19916.

6 L. Hao, X. Liu, D. Zhai, L. Qiu, C. Ma, P. Ma and J. Jiang, Theoretical Studies on the Performance of HMX with Different Energetic Groups, *ACS Omega*, 2020, **5**, 29922–29934.

7 H. Wei, C. He, J. Zhang and J. M. Shreeve, Combination of 1,2,4-Oxadiazole and 1,2,5-Oxadiazole Moieties for the Generation of High-Performance Energetic Materials, *Angew. Chem., Int. Ed*., 2015, **54**, 9367–9371.

8 (a) P. Yin, J. Zhang, G. H. Imler, D. A. Parrish and J. M. Shreeve, Polynitro-Functionalized Dipyrazolo-1,3,5-triazinanes: Energetic Polycyclization toward High Density and Excellent Molecular Stability, *Angew. Chem., Int. Ed*., 2017, **56**, 8834–8838; (b) J. Zhang, P. Yin, L. A. Mitchell, D. A. Parrish and J. M. Shreeve, N-Functionalized Nitroxy/Azido Fused-Ring Azoles as High-Performance Energetic Materials, *J. Mater. Chem. A*, 2016, **4**, 7430–7436.

9 (a) W. Zhang, J. Zhang, M. Deng, X. Qi, F. Nie and Q. Zhang, A Promising High-Energy-Density Material, *Nat. Commun*., 2017, **8**, 181; (b) P. Yin and J. M. Shreeve, Nitrogen-Rich Azoles as High Density Energy Materials, *Adv. Heterocycl. Chem*., 2017, **121**, 89–131; (c) L. L. Fershtat and N. N. Makhova, 1,2,5-Oxadiazole-Based High-Energy-Density Materials: Synthesis and Performance, *Chempluschem*, 2020, **85**, 13–42.

10 K. Mohammad, V. Thaltiri, N. Kommu and A. A. Vargeese, Octanitropyrazolopyrazole: A Gem-Trinitromethyl Based Green High-Density Energetic Oxidizer, *Chem. Commun*., 2020, **56**, 12945–12948.

11 G. Zhao and M. Lu, Theoretical Studies on the Structures and Detonation Properties of Nitramine Explosives Containing Benzene Ring, *J. Mol. Model*., 2012, **18**, 2443–2451.

12 V. D. Ghule, A. Nirwan and A. Devi, Estimating the Densities of Benzene-Derived Explosives Using Atomic Volumes, *J. Mol. Model*., 2018, **24**, 50.

13 J. H. Boyer and R. S. Buriks, 2,4,5-Triaminonitrobenzene, *Organic Syntheses*, John Wiley & Sons, Inc., Hoboken, NJ, USA, 2003, 96–96.

14 M. A. Spackman and J. J. McKinnon, Fingerprinting Intermolecular Interactions in Molecular Crystals, *CrystEngComm*, 2002, **4**, 378–392.

15 M. A. Spackman and D. Jayatilaka, Hirshfeld surface analysis, *CrystEngComm*, 2009, **11**, 19–32.

16 (a) T, Lu, F. Chen, Multiwfn: A multifunctional wavefunction analyzer, *J. Comput. Chem*., 2012, **33**, 580–592; (b) E. R. Johnson, S. Keinan, P. Mori-Sánchez, J. Contreras-García, A. J. Cohen and W. Yang, Revealing Noncovalent Interactions, *J. Am. Chem. Soc.*, 2010, **132**, 6498–6506; (c) W. Humphrey, A. Dalke and K. Schulten, VMD: Visual Molecular Dynamics, *J. Mol. Graph.*, 1996, **14**, 33–38.

17 R. Mayer, J. Köhler and A. Homburg, *Explosives*, WileyVCH, Weinheim, Germany, 6th edn, 2007.

18 Y. Tang, C. He, L. A. Mitchell, D. A. Parrish, and J. M. Shreeve, C–N Bonded Energetic Biheterocyclic Compounds with Good Detonation Performance and High Thermal Stability, *J. Mater. Chem. A*, 2016, **4**, 3879-3885.

19 M. J. Frisch, et al. *Gaussian 03, Revision E.01* Gaussian, Inc. 2004.

20 G. M. Sheldrick, SHELXT – Integrated Space-Group and Crystal-Structure Determination, *Acta Crystallogr. Sect. C Struct. Chem*., 2015, **71**, 3–8.

21 G. M. Sheldrick, Crystal Structure Refinement with SHELXL, *Acta Crystallogr. Sect. A Found. Adv*., 2015, **71**, 3–8.

22 O. V. Dolomanov, L. J. Bourhis, R. J. Gildea, J. A. K. Howard and H. Puschmann, OLEX2 : A Complete Structure Solution, Refinement and Analysis Program, *J. Appl. Crystallogr*., 2009, **42**, 339–341.

23 R. G. Parr and W. Yang, Density Functional Theory of Atoms and Molecules, *Oxford University Press*, New York, 1989.

24 O. M. Suleimenov and T. K. Ha, Ab Initio Calculation of the Thermochemical Properties of Polysulphanes (H2Sn), *Chem. Phys. Lett*., 1998, **290**, 451.

25 H. D. B. Jenkins, D. Tudela and L. Glasser, Lattice Potential Energy Estimation for Complex Ionic Salts from Density Measurements, *Inorg. Chem*., 2002, **41**, 2364.

26 M. S. Westwell, M. S. Searle, D. J. Wales and D. H. Williams, Empirical Correlations between Thermodynamic Properties and Intermolecular Forces, *J. Am. Chem. Soc*., 1995, **117**, 5013.